

Tropical cyclones facilitate recovery of forest leaf area from summer droughts in East Asia

Yi-Ying Chen¹ and Sebastiaan Luyssaert²

¹Research Center for Environmental Changes, Academia Sinica, Taipei, 11529, Taiwan

²Faculty of Science, Vrije Universiteit Amsterdam, Amsterdam, 1081, The Netherlands

Correspondence to: Yi-Ying Chen (yiyingchen@gate.sinica.edu.tw)

Abstract. Forests disturbance by tropical cyclones is mostly documented by field studies of exceptionally strong cyclones and satellite-based approaches attributing decreases in leaf area. By starting their analysis from the observed damage, these studies are biased and may, therefore, limit our understanding of the impact of cyclones in general. This study overcomes such biases by jointly analysing the cyclone tracks, climate reanalysis, and changes in satellite-based leaf area following the passage of 140 ± 41 cyclones. Sixty days following their passage, 18 ± 8 % of the cyclones resulted in a decrease and 48 ± 18 % showed no change in leaf area compared to nearby forest outside the storm track. For a surprising 34 ± 7 % of the cyclones, an increase in leaf area was observed. Cyclones resulting in higher leaf area in their affected compared to their reference area coincided with an atmospheric pressure dipole steering the cyclone towards a region experiencing summer drought caused by the same dipole. When the dipole was present, the destructive power of cyclones might have been offset by their abundant precipitation enabling forest canopies in the affected area to recover faster from the drought than canopies in the reference area. This study documents previously undocumented wide-spread antagonist interactions on forest leaf area between droughts and tropical cyclones.

Main Text

Each year almost 30 cyclones, about one-third of the world's tropical cyclones, develop over the Pacific Ocean north of the equator (Landsea, 2000) where a subtropical ridge steers them mainly west and northwest towards Eastern Asia, where 90 % make landfall. The majority of the tropical cyclones in the north western Pacific basin develop between June and November (Bushnell et al., 2018) and more than half acquire typhoon strength (WMO, 2017). The four most powerful typhoons in the region since 1999, i.e., Morakot in 2009, Megi in 2010, Haiyan in 2013, and another typhoon also named Megi in 2016, claimed over 7,000 lives, left 1,700 missing, and destroyed over 10 billion USD worth of infrastructure and crops according to compilations of mostly local news sources (Yang et al., 2014; Bowen, 2016; Lu et al., 2017; OCHA, 2010). Although natural ecosystems, such as forests, have adapted to recurring high wind speeds (Eloy et al., 2017; Louf et al., 2018; Curran et al., 2008), stem breakage is almost unavoidable at wind speeds above 40 m s^{-1} (Virot et al., 2016) but has been widely reported at wind speeds well below this threshold together with other damage (Tang et al., 2003; Chiu et al., 2018; Chang et al., 2020). Despite

32 the economic importance of forests in the region (Barbier, 1993; Vickers et al., 2010), an overall assessment of the
33 damage of tropical cyclones on forest resources is still lacking.

34
35 By jointly analysing cyclone tracks (Joint Typhoon Warning Center ; JTWC, 2019), climate reanalysis data (ERA5-
36 Land; ECMWF, 2019), satellite-based proxies of soil dryness (SPEIbase v2.6; Beguería et al., 2014), land cover
37 (ESA CCI; ESA, 2017), and leaf area (ESA LAI; Martins et al., 2020), we estimated: (a) the potential forest area
38 damaged by tropical cyclones, (b) the impact of tropical cyclones on leaf area, and (c) the main drivers of this
39 impact. Previous studies attributed decreases in leaf area or related satellite-based indices to different disturbance
40 agents (Ozdogan et al., 2014; Honkavaara et al., 2013; Forzieri et al., 2020), including cyclones (Takao et al., 2014).
41 A damage-based approach is designed to identify only decreases in leaf area, thus failing to identify events in which
42 tropical cyclones left the leaf area unaltered or even increased it. In contrast, this study starts the analysis from the
43 actual storm tracks which allows for an unbiased assessment of the impact of cyclones on forests (Blanc and Strobl,
44 2016).

45
46 The land area affected was identified for each of the 580 tropical cyclones that occurred in the study region between
47 1999 and 2018, considering that cyclone-driven damage could only occur within the storm track at locations that
48 experienced high wind speeds or high precipitation. Pixels within the storm track defined as 2, 3 or 4 times the
49 diameter of the cyclone for which threshold values for wind or precipitation were exceeded were classified as
50 affected areas, the remaining pixels in the track served as a cyclone-specific reference area. The uncertainty derived
51 from defining the width of the storm track (Willoughby and Rahn, 2004) and determining which wind speeds and
52 amounts of precipitation could result in damage are accounted for by an ensemble of nine related definitions with
53 different threshold values (**Table A1**). In this report uncertainties represent the standard deviation across the nine
54 definitions for the affected area and are accounted for in Figs 1, 2, 3, and A2, and Tables A1, A2 and A3.

55
56 Since 1999, $2,240,000 \pm 690,000$ km² of forest in the study region experienced conditions that may have resulted in
57 cyclone-driven damage, at least once every decade (**Fig. 1a**). At decadal or longer return intervals, a single cyclone
58 may greatly affect ecosystem functioning, forest structure and species composition of the forest (Xi, 2015;
59 Castañeda-Moya et al., 2020). No less than $540,000 \pm 260,000$ km², including 70 % of the tropical forest in the
60 region, experienced potentially damaging conditions at least once per year, and are thus classified as being under
61 chronic wind stress (**Fig. 1b**). Estimates from the rain-only definitions closely matched the $700,000$ km² yr⁻¹ that was
62 reported following a similar approach in which the affected area was defined as a 100 km buffer zone along the
63 storm track (Lin et al., 2020).

64
65 Irrespective of the definition of the affected area, the coefficient of variation of the between-year variation in
66 potentially damaged areas ranged from 15 to 20 % (**Fig. 1c**). Excluding the four most powerful typhoons that
67 occurred in the region since 1999 changed the average coefficient of variation from 17 to 16 %. This suggests that

68 the most powerful typhoons make only a small contribution to the total annually potentially affected area in the
69 region. A recent literature review reported, however, that 66 % of the research papers in this area have examined the
70 effects of only about 6 % of the most powerful cyclones (Lin et al., 2020). The relatively small contribution of those
71 events to the potentially damage area suggests that in regions with frequent tropical storms, disturbance ecology
72 would benefit from broadening its scope by examining the effects and recovery of a representative sample of
73 tropical cyclones, rather than focusing on the most devastating events.

74
75 The impact of a tropical cyclone on leaf area was calculated based on the adjusted Hedge's effect size by comparing
76 the change in leaf area before and after the cyclone in the affected area with the change before and after the cyclone
77 in the reference area for each individual cyclone (**Eq. 1**). Using a reference area that is specific to each cyclone
78 means that seasonal dynamics related to leaf phenology and seasonal monsoons are accounted for in the effect size,
79 which is a unitless description of the mean change in leaf area normalized by its standard deviation (**Eq. 1**). Hence, a
80 positive effect size denotes a faster increase or a slower decrease in leaf area in the affected area compared to the
81 reference area following the passage of a tropical cyclone.

82
83 A total of 316 ± 22 tropical cyclones or 54 ± 4 % of the storm events under study could not be further analysed
84 (**Table A1**) because leaf area index observations were missing from either the affected area, the reference area, or
85 both, thus violating the requirements for calculating the effect size (**Eq. 1**). Of the remaining 264 ± 22 tropical
86 cyclones, only 140 ± 41 passed the additional quality check necessary to be retained for further analysis in this study,
87 i.e., the difference in the leaf area between the reference and affected area prior to the passage of a storm should be
88 less than 10 % of the leaf area in the reference area. In other words, prior to the storm, the leaf area in the reference
89 area had to be similar to the leaf area in what will become the affected area once the storm passed. Of the 580
90 cyclones, 31 % was less than class 1, 14 % was classified as class 1, 11 % as class 2, 10 % as class 3, 21 % as class
91 4, and 13 % as class 5. The distribution of the intensity classes of the sample of 140 ± 41 cyclones that could be
92 further analysed were similar to the census of the 580 cyclones with 33 % of the retained cyclones classified below
93 class 1, 13 % in class 1, 8 % in class 2, 9 % in class 3, 23 % in class 4, and 14 % class 5. Despite the loss of around
94 75 % of the 580 events, the sample analysed in this study is unbiased in terms of cyclone intensity classes (**Fig. A2**).

95
96 Tropical cyclones have been widely observed to defoliate and disturb forests because of limb breaking, uprooting,
97 stem breakage and landslides following high wind speeds and heavy precipitation (Wang et al., 2013; Uriarte et al.,
98 2019; Chambers et al., 2007; Douglas, 1999; Lin et al., 2011). Nevertheless, in this study, only 18 ± 8 % of the
99 observed cyclones resulted in a detectable reduction in leaf area 60 days after their passage as a direct effect of limb
100 breakage, uprooting, stem breakage and landslides. For 48 ± 18 % of the cyclones, the change in leaf area 60 days
101 after a cyclone passed was so small that it could not be distinguished from the threshold representing no-change.
102 Ecological theory predicts forest dwarfing in regions with high cyclone frequencies compared to the longevity of a
103 tree, directly through gradual removal of taller trees over many generations (Lin et al., 2020; McDowell et al., 2020)

104 and indirectly through the loss of nutrients (Tang et al., 2003; Lin et al., 2011). Where forest dwarfing has occurred,
105 it might be hard to observe the short-term effects of an individual tropical cyclone on forest structure and function
106 (Mabry et al., 1998).

107
108 For a surprising 34 ± 7 % of the cyclones an increase or given the way the effect size was calculated, a reduced
109 decrease in leaf area was observed, leading to the question which conditions lead to an increase or a reduced
110 decrease in leaf area between the affected and reference areas 60 days following the passage of a tropical cyclone?
111 To answer this question, two groups of meta-data were compiled for each of the 140 ± 41 tropical cyclones that
112 passed the quality checks, the first group consisting of five characteristics describing the land surface before the
113 passage of a cyclone and the second group containing five characteristics of the cyclone itself (**Table A2**).
114 Following factorial analysis to identify collinearity between the meta-data in the same group, the explanatory power
115 of the meta-data was quantified as a decrease in the accuracy of a random forest analysis (**Fig. 2**). The random forest
116 analysis was repeated 12 times with different combinations of largely uncorrelated meta-data (**Table A3**). Each
117 random forest analysis included the effect sizes and meta-data for all nine definitions of affected area to account for
118 this specific source of uncertainty.

119
120 The statistical analysis showed that accumulation of precipitation during the passage of a cyclone over land makes
121 the largest contribution to the accuracy of the random forest analysis. Randomizing this variable decreased the
122 accuracy of the random forest analysis by 9 to 21 % (**Fig. 2**). The Pacific Japan index for atmospheric pressure at the
123 time of landfall was the second most important variable contributing 1 to 17 %. The other meta-data contributed
124 relatively little (-6 to 8 %) to the accuracy of the random forest analysis with negative importance indicating that
125 removing the variable from the model improved its performance. Subsequently, the six meta-data with the highest
126 explanatory power were used to build a single regression tree to obtain the environmental drivers and their cut-off
127 values that would best explain the change in leaf area following the passage of a tropical cyclone (**Fig. 3**). Note that
128 cyclone intensity had a low explanatory power (**Fig. 3**) which is explained by the observation that positive, neutral
129 and negative effects occurred in all five intensity classes (**Fig. A2**). The remainder of this report focusses on the
130 mechanisms underlying the increase or reduced decrease in leaf area following the passage of a tropical cyclone.

131
132 Cyclones bringing abundant precipitation (> 32 mm) during summer months (i.e., after month 6.5) when the
133 atmosphere was under a positive phase of Pacific Japan index (> -0.028) resulted dominantly (56 % to 69 %) in a
134 leaf area that was $0.5 \text{ m}^2 \text{ m}^{-2}$ higher in the affected compared to the reference area (**Fig. 3**). Given that the passage of
135 the cyclone was often preceded by a summer drought, the observed increase in leaf area should most likely be
136 interpreted as a faster recovery from the drought in the area affected by the cyclone than in its reference area. The
137 vegetation response was thought to be the outcome of two elements: (a) cyclones making landfall in June, July and
138 August bring 30 to 50 % of the annual precipitation in coastal areas in the study domain (**Fig. A3**) and are thus
139 substantial sources of precipitation. The importance of the precipitation brought by tropical cyclones is confirmed by

140 domain-wide changes in the standardized precipitation-evapotranspiration index showing that 1006 of the 1262 (80
141 %) cyclones increased soil wetness, and (b) given that much of the study domain has a monsoon climate with
142 relatively little rain in the fall and winter months (Chou et al., 2009), the implication is that summer droughts might,
143 for evergreen vegetation, have lasting effects until the next growing season unless the drought is ended before the
144 dry season begins.

145
146 An increase in leaf area or a reduced decrease, following the passage of a tropical cyclone, thus requires three
147 conditions to co-occur: (a) a dry spell, (b) a cyclone making landfall in the region experiencing the dry spell, and (c)
148 the cyclone bringing abundant precipitation to mitigate the soil dryness. At first sight, meeting all three conditions at
149 the same time seems unlikely, however, for the mid-latitudes, including Korea, China, Taiwan, and Japan, dry
150 summers see an increase in the number of tropical cyclones making landfall which often end the summer drought
151 (Yoo et al., 2015). In South Korea, for example, at least 43 % but possibly as much as 90 % of the summer droughts
152 in coastal regions were abruptly ended by a tropical cyclone (Yoo et al., 2015). Based on our analysis of the
153 standardized precipitation-evapotranspiration index, at least 210 of the 1262 (17 %) tropical cyclones in East Asia
154 ended a drought.

155
156 The co-occurrence of dry spells and tropical cyclones has been linked to a meridional dipole system in the mid-
157 latitude regions of East Asia with a high pressure system in the region of 40-50 N and 150-160 E where it is causing
158 the dry spell, and the low pressure system in the region of 20-30 N and 120-150 E. When such a dipole exists,
159 tropical cyclones generated from the monsoon trough over the West Pacific Ocean are steered through the trough in
160 between the high- and low-pressure systems towards and then along the coast of East Asia (Choi et al., 2010). While
161 travelling along the edges of the high pressure system, the tropical cyclone may disturb the circulation, resulting in
162 an unfavourable environment to sustain the dipole (Choi et al., 2011; Kubota et al., 2016) and bringing precipitation
163 to the dry region that was under the high pressure system.

164
165 As suggested by the random forest analysis (**Fig. 2**), analysing the atmospheric pressure separately for cyclones that
166 resulted in no change, an increase or a decrease in leaf area (**Fig. 4**) showed that tropical cyclones that were
167 followed by an increase or reduced decrease in leaf area coincided with a meridional dipole (**Fig. 4b**). Moreover, the
168 genesis of tropical cyclones that were followed by a decrease in leaf area, occurred under very different atmospheric
169 conditions compared to cyclones followed by an increasing leaf area. A relationship between the atmospheric
170 system causing summer droughts, tropical cyclones and their subsequent impact on leaf areas, suggest that whether
171 more drought damage is to be expected in the future will not only depend on an increase in drought frequency and
172 intensity but will in part be determined by the exact weather system that is causing the drought. Although the co-
173 occurrence of droughts and cyclones has previously been demonstrated (Choi et al., 2011; Kubota et al., 2016), we
174 believe to be the first to document its large-scale antagonist effect on forest leaf area.

175

176 By studying a representative sample of tropical cyclones in terms of storm intensity (**Fig. A2**), we have shown that
177 almost half of the tropical cyclones, i.e., $48 \pm 18 \%$, caused little to no damage to forest leaf area, suggesting that
178 forest dwarfing is a general structural adaptation in the study region. Moreover, a third, i.e., $34 \pm 7 \%$ of the cyclones
179 in East Asia resulted in an increase or reduced decrease in forest growth, because these storms relieved water stress
180 within their track or even ended summer droughts. The observed frequency of positive vegetation responses to
181 cyclones suggests that the present day vision of cyclones as agents of destruction (Altman et al., 2018; Negrón-
182 Juárez et al., 2010, 2014) should be refined toward a recognition that, depending on the environmental conditions
183 prior to the storm and the atmospheric conditions leading to the genesis of the tropical cyclone, cyclones frequently
184 facilitate the recovery of forest leaf area and as such dampen the effects of summer droughts.

185

186 **Materials and Methods**

187 **Cyclone track and track diameter**

188 Since 1945, tropical cyclones in the Western North Pacific Ocean have been tracked and their intensity recorded by
189 the Joint Typhoon Warning Center (JTWC). The track data shared by the Joint Typhoon Warning Center consist of
190 quality-controlled six-hourly geolocation observations of the centre of the storm with the diameter of the storm
191 being a proxy for its intensity (JTWC, 2019). For the period under consideration, from 1999 to 2018, the
192 geolocations and diameters are the output of the Dvorak model (Dvorak, 1984; Dvorak et al., 1990) derived from
193 visible and infrared satellite imagery. Storm diameters are available starting from January 2003. Prior to this date a
194 generic diameter of 100 km (Lin et al., 2020) is used in this study. Linear interpolation of the six-hourly track data
195 resulted in hourly track data to fill in any gaps in the mapping of the cyclone track.

196

197 In this study, we focus on East Asia which, given the absence of natural boundaries, is defined as the land contained
198 within the north western Pacific basin that, according to the Joint Typhoon Warning Center stretches from 100 to
199 150 degrees east and 0 to 60 degrees north. The Joint Typhoon Warning Center compiled track and intensity data for
200 580 tropical cyclones between 1999 and 2018 in the north western Pacific basin. A shorter time series (1999 to 2018)
201 than the entire length of time available (1945 to 2018) was analysed due to the more limited availability of the leaf
202 area index data which had to be jointly analysed with the track and intensity data to quantify the impact of cyclones
203 on natural ecosystems.

204

205 **Area affected by individual cyclones**

206 The land area thought to be affected by a specific cyclone as well as the reference area for each of the 580 cyclones
207 that occurred in the study area between 1999 and 2018 were identified based on nine different but related definitions
208 (**Table A1**). Each definition comprises a combination of at least two out of three criteria, e.g., the diameter of the
209 cyclone, the maximum wind speed at each location during the passage of the cyclone and accumulated precipitation
210 at each location during the passage of the cyclone. Each forested pixel within each individual storm track was

211 classified as either affected area or reference area based on these nine definitions. Differences in the results coming
212 from differences in the definitions were used throughout the analysis to estimate semantic uncertainties.
213 Uncertainties related to the estimated diameter of the cyclone, wind speed and precipitation data were not accounted
214 for in the calculation of the affected and reference areas because they were thought to be smaller than the uncertainty
215 coming from differences in the definitions themselves.

216
217 The underlying assumption behind the definitions is that forests can only be affected by a specific cyclone if they are
218 located along its storm track. The minimum width of each storm track is the diameter of the cyclone as reported by
219 the Joint Typhoon Warning Center. Following the observation that over the ocean, the actual wind speed exceeds the
220 critical wind speed for stem breakage or uprooting (i.e., 17 m s^{-1} ref. Chen et al., 2018) over a distance of at least
221 three times the diameter of the cyclone (Willoughby and Rahn, 2004), the minimum width of a storm track in which
222 cyclone-related forest damage could occur is defined as three times the diameter recorded by the Joint Typhoon
223 Warning Center although wind speeds drop dramatically when cyclones make land fall (Kaplan and Demaria, 2001).
224 The minimum width of a storm track over land should, therefore, be reduced compared to the observations over the
225 ocean. This study used three different widths to define a storm track, i.e., two, three or four times the recorded
226 diameter (**Table A1**).

227
228 Being located within the track of a specific cyclone is essential but not sufficient for damage to occur. Within a
229 storm track, only forested pixels that experienced high wind speeds or high precipitation were counted as in the
230 potentially affected area. Forest pixels that were located within the storm track but did not experience high wind
231 speeds or high precipitation were counted as in the reference area. Note that to better account for the uncertainties
232 arising from this approach, the threshold values for wind speed and precipitation were increased as the track
233 diameter increased (**Table A1**). For a narrow storm track it is reasonable to assume that there would be damage
234 shown in all pixels except those where wind speed or precipitation did not exceed a relatively low threshold value.
235 For wide storm tracks the opposite applies; it is reasonable to assume that few of the pixels would show damage
236 except where wind speed or precipitation exceeded relatively high threshold values.

237
238 Wind speed and precipitation data were extracted from the ERA5-Land reanalysis data for land (ECMWF, 2019).
239 The ERA5-Land reanalysis dataset has a spatial resolution of $9 \text{ km} \times 9 \text{ km}$ and a time step of 1 hour. It is the product
240 of a data assimilation study conducted with the H-TESEL scheme by ERA5 IFS Cy45r1 and nudged by
241 climatological observations (ECMWF, 2018). The Cy45r1 reanalysis dataset shows statistically neutral results for
242 the position error of individual cyclones (ECMWF Confluence Wiki: Implementation of IFS cycle 45r1). The spatial
243 representation of the reanalysis data is reported to compare favourably with observational data (Chen et al., 2021)
244 outside the domain of this study. No reports on similar tests for the current study domain, i.e., East Asia, were found.
245 Furthermore, land cover maps released through the European Space Agency's Climate Change Initiative (ESA, 2017)
246 were used to restrict the analysis to forests. The Climate Change Initiative maps integrate observations from several

247 space-borne sensors, including MERIS, SPOT-VGT, AVHRR, and PROBA-V, into a continuous map with a 300 m
248 resolution from 1994 onwards.

249
250 Wind speed and precipitation data were spatially disaggregated and temporally aggregated to match the spatial and
251 temporal resolution of the leaf area index product (see below). Maximum wind speed and accumulative precipitation
252 were aggregated over time steps to match the 10-day resolution of the leaf area index product. We preserved the
253 temporal resolution of the land cover map but aggregated its spatial resolution from 300 m to 1 km to match the
254 resolution of the leaf area index product. During aggregation, the majority of land cover at the 300 m resolution was
255 assigned to the 1 km pixel resolution.

256
257 **Impact on leaf area of an individual cyclone**

258 Version 2 of European Space Agency’s Climate Change Initiative product was used to calculate leaf area in this
259 study. The product has a 1 km spatial resolution, a 10-day temporal resolution, and is available from 1999 onwards.
260 The default leaf area index product is distributed as a composite image using at least six valid observations on a
261 pixel within a 30-day moving window (Verger et al., 2014). The composite image is drawn from satellite-based
262 observations of the surface reflectance in the red, near-infrared, and shortwave infrared from SPOT-VGT (from
263 1999 to May 2014) and PROBA-V (from June 2014 to present). Gaps in missing observations are filled by the
264 application of a relationship between local weather and leaf area index dynamics. Gap filling resulted in errors on
265 the leaf area index estimates of less than 0.18 (Martins et al., 2017). The spatiotemporal resolution of the leaf area
266 index products was the coarsest of all data products used and therefore determined the spatiotemporal resolution of
267 the analysis as a whole. Moreover, the availability of the leaf area index product determined the starting date for the
268 study.

269
270 The impact of cyclones on leaf area was calculated by comparing the change in leaf area before and after the
271 cyclone in the affected area with changes before and after the cyclone in the reference area for each individual
272 cyclone. In this approach, the reference area serves as the control for the affected area, given that reference area and
273 the affected area may have a different size, the adjusted Hedge’s effect size (Rustad et al., 2001) can be used to
274 calculate the effect size of an individual cyclone on leaf area (**Eq. 1**). Using a reference area that is specific to each
275 cyclone, seasonal dynamics such as leaf phenology, are accounted for in the effect size. Effect size is thus a unitless
276 quantifier which describes the mean change in state, obtained by normalizing the mean difference in leaf area with
277 the standard deviation (**Eq. 1**). A positive or negative effect size value indicates, respectively, an increase or
278 decrease in leaf area following the passage of a cyclone:

279
280
$$ES = \frac{(\overline{LAI}_{bef} - \overline{LAI}_{aft})_{afj} - (\overline{LAI}_{bef} - \overline{LAI}_{aft})_{ref}}{\sigma}, \quad [1]$$

281

282 where ES is the event-based effect size for leaf area. The upper bar represents the mean of leaf area index in the
283 reference (*ref*) or the affected (*aff*) area. The subscripts *bef* and *aft* denote the observation dates before and after the
284 cyclone; σ denotes the standard deviation of all observations within the storm track. Given the 10-day frequency of
285 the ESA leaf area index product, two leaf area index maps are used for the calculation of the effect size, one to
286 characterize the leaf area index 1 to 10 days before the cyclone and the other to characterize the leaf area index 60 to
287 70 days after the cyclone. To distinguish between the affected and reference areas the effect sizes were calculated
288 for each event using the nine definitions. After applying the quality control criteria (see below) a different number of
289 events was available for each definition (**Table A1**).

290
291 Starting the analysis from the actual storm tracks, as was the case in this study, allows for an unbiased assessment of
292 the impact of cyclones on forests (Blanc and Strobl, 2016), in contrast to studies that attribute decreases in leaf area
293 or related satellite-based indices to different disturbance agents (Ozdogan et al., 2014; Honkavaara et al., 2013;
294 Forzieri et al., 2020) including cyclones (Takao et al., 2014). By design, the latter approach is not capable of
295 identifying neutral or positive impacts of cyclones on leaf area. As positive effects were not limited to the cyclones
296 from a low intensity class (**Fig. A2**), the intensity class had little explanatory power (**Fig. 2**) making a systematic
297 bias towards positive effect sizes caused by low intensity cyclones unlikely. Given the 60-day time window, our
298 method is more likely to be biased towards detecting no changes in leaf area than detecting positive or negative
299 changes in leaf area.

300
301 A meaningful effect size relies on the change in the reference area to evaluate whether the change in leaf area in the
302 affected area is faster, similar or slower. The way the effect size is calculated thus accounts for phenological changes
303 in leaf area. If the reference area would not be used in the calculation of the effect size, the change in leaf area over
304 the affected area would mostly represent leaf phenology especially if the 60-day window includes the start or the
305 end of the growing season, and would thus be unsuitable to address the question at hand.

306
307 As this study aims to quantify changes in leaf area index, it could not make use of gap filled leaf area index values
308 which would level off such changes. Furthermore, calculating the effect size required leaf area index estimates
309 before the passage of the cyclone in the reference and soon-to-be affected area and leaf area index estimates after the
310 passage of the cyclone in the reference and affected area. The 60-day time frame was a compromise to avoid
311 excessive data gaps in the leaf area index product when using the composite leaf area index product. Because the
312 leaf area index product reports leaf area index values within a 60-day window, the analysis had to be refined so that
313 this 60-day window never included the cyclone. The offset between the cyclone and a leaf area index observation
314 from the composite leaf area index product was calculated by subtracting the date of the cyclone from the last
315 observation date of the leaf area index composite data before the cyclone or first observation date of the leaf area
316 index composite data after the cyclone. Pixels with a negative offset indicated that the composite data were likely to

317 include observations from both before and after the cyclone and were therefore discarded in the calculations of the
318 effect size.

319

320 The calculation of the effect size assumes having a similar leaf area index between the area that will become the
321 affected area and the area that will become the reference area after the passage of a cyclone. If the absolute
322 difference in leaf area index between the reference and the affected area was less than 10 %, the effect size
323 calculated for this event was included in subsequent analyses. This can be formalized as:

324

$$325 \left| \frac{\overline{LAI}_{beff}}{\overline{LAI}_{befref}} - 1 \right| < 0.1 \quad [2]$$

326

327 Where the 0.1 represents the 10 % threshold that was guided by the observed relationship between the remotely-
328 sensed leaf area and its deviation to ground truth data for leaf areas of 5 m² m⁻² or below (Fig. 26 in Jorge, 2020).
329 This quality control criterion reflects the idea that prior to the passage of a tropical cyclone, the LAI needs to be
330 similar in what will become the reference and affected area. If not, changes in leaf area following the passage of the
331 cyclone cannot be assigned to its passage.

332

333 Following the passage of a tropical cyclone, a change in LAI of less than 10% before and after the passage of the
334 cyclone was, in line with the quality control criterion, considered to be too small to be considered substantial. Such
335 events were classified as cyclones with a neutral effect size. This classification was formalized as:

336

$$337 \left| (\overline{LAI}_{bef} - \overline{LAI}_{aft})_{aff} - (\overline{LAI}_{bef} - \overline{LAI}_{aft})_{ref} \right| < 0.1 * (\overline{LAI}_{bef})_{ref} \quad [3]$$

338

339 **Multivariate analysis**

340 Each tropical cyclone was characterized by its: (1) latitude of landfall (degrees); (2) intensity of the tropical cyclone
341 (m s⁻¹); (3) month of landfall; (4) maximum wind speed during passage over land (m s⁻¹); (5) accumulated rainfall
342 during passage over land (mm); (6) accumulated rainfall on land 30 days prior to landfall of the cyclone (mm); (7)
343 affected area during passage over land (km²); (8) leaf area 30 days prior to landfall (m² m⁻²); (9) Standardized
344 Precipitation Evapotranspiration Index (mm mm⁻¹) as a drought proxy; and (10) Pacific Japan index the month of
345 landfall (Pa Pa⁻¹). These characteristics were calculated as the average along the trajectory of the cyclone.

346

347 Characteristics 1 to 4 were retrieved from the Joint Typhoon Warning Center database as detailed in ‘Cyclone track
348 and track diameter’. Characteristics 5 to 6 were retrieved from the ERA5-Land reanalysis data for land (ECMWF,
349 2019) and characteristic 7 from the analysis combining cyclone track, cyclone diameter and ERA5-Land reanalysis,
350 as explained in ‘Area affected by individual cyclones’. Characteristic 8 was taken from the leaf area index analysis
351 as explained in ‘Impact on leaf area of an individual cyclone’. For characteristic 9, the Standardized Precipitation

352 Evapotranspiration Index was used and combined with the cyclone masks created in ‘Area affected by the individual
353 cyclone’. Characteristic 10, the Pacific Japan index, was calculated from ERA5 hourly reanalysis (Hersbach et al.,
354 2018). Details on the calculation of characteristics 9 and 10 are provided in subsequent sections.

355
356 These ten characteristics were separated into two groups describing the condition of the land and ocean prior to the
357 event and the characteristics of the tropical cyclone itself. The prior conditions group contained: pre-event leaf area
358 index, pre-event drought state, pre-event accumulative rainfall, oceanic Nino index, and month. Characteristics such
359 as maximum wind speed, accumulative rainfall, cyclone intensity, affected area, and latitude were used to describe
360 the cyclone itself (**Table A2**).

361
362 Factor analysis (Grice, 2001) was used to reveal the collinearity among the selected variables in the prior conditions
363 and tropical cyclone characteristic group (**Table A2**). Collinearity was used to create 12 sets (4 x 3) of mostly
364 independent characteristics (**Table A3**) which were used as the input for a random forest tree to identify the
365 characteristics that best explained the effect size for leaf area index. The random forest analysis was repeated for
366 each of the 12 sets, but limited to four-layer random forest trees, to identify the importance of the environmental
367 variables on the tropical cyclone effect size (not shown). Finally, to reduce the collinearity of the input variables,
368 only the six variables with the highest accuracy in the random forest were used to create a single decision tree which
369 is shown in **Fig. 3**. For this, the recursive partitioning approach was used with a maximum of four levels and a
370 minimum of 20 samples in each node provided by the R-rpart package (Therneau et al., 2019).

371 372 **Drought analysis**

373 The standardized precipitation evapotranspiration index, is a proxy index for drought that represents the climatic
374 water balance and was used to assess the drought of a forest soil before and after the passage of an individual
375 tropical cyclone. The standardized precipitation evapotranspiration index data between 1999 and 2018 were
376 retrieved from the Global Standardized Precipitation and Evapotranspiration Index Database (SPEIbase v2.6
377 (Beguería et al., 2014)), which is based on the CRU TS v.4.03 dataset (Harris et al., 2020). In this study, the
378 temporal resolution of the data was preserved but the spatial resolution was regridded from the original half-degree
379 to 1 km to match the resolution of the ESA leaf area index product. The contribution of an individual tropical
380 cyclone to ending a drought was evaluated by comparing the standardized precipitation and evapotranspiration index
381 from affected and reference areas through the following equation:

$$382 \quad \delta SPEI = (SPEI_{imon})_{aff} - (SPEI_{imon})_{ref}, \quad [3]$$

384
385 where $\delta SPEI$ is the event-based change in standardized precipitation and evapotranspiration index. A positive or
386 negative $\delta SPEI$ respectively denotes an increase or decrease in available water resources following the passage of a
387 tropical cyclone. The subscription *imon* represents the integration time of available water resources in the

388 calculation of the standardized precipitation and evapotranspiration index either in the reference (*ref*) or the affected
389 (*aff*) area which are defined in previous section. The same time window, i.e., 60-days, was applied for the
390 calculation of δ SPEI and event-based effect size for leaf area index.

391

392 **Atmospheric analysis**

393 The Pacific Japan index was calculated by comparing the difference of the 3-month running mean atmospheric
394 pressure anomaly from Yokohama in Japan (35 N, 155 E) with Hengchun in Taiwan (22.5 N, 125 E) (Kubota et al.,
395 2016) with the 20 year climatology from 1999 to 2019. A monthly Pacific Japan index was used in this study and
396 the pressure data were retrieved from ERA5 (Hersbach et al., 2018).

397

398 The Pacific Japan index for the month of the passage of each tropical cyclone were stratified according to the impact
399 (given by the effect size) of the cyclone on forest leaf area. Mean absolute atmospheric pressure field and leaf area
400 were calculated for those cyclones with a neutral effect size on leaf area (**Fig. 4a**). Changes in pressure field and leaf
401 area were calculated for both cyclones with a positive and negative impact on leaf area (**Fig. 4b & c**).

402

403

404 **Acknowledgments**

405 Y.Y.C. would like to thank the National Center for High-performance Computing (NCHC) for sharing its
406 computational resources and data storage facilities. Y.Y.C. was funded through the Ministry of Science and
407 Technology (grant MOST 109-2111-M-001-011 and grant MOST 110-2111-M-001 -011).

408

409

410 **Data availability**

411 R-Scripts and data for performing the analysis and creating the plots can be found at
412 https://github.com/ychenatsinca/LAI_STUDY_EA_V1/releases/tag/v1 and <https://doi.org/10.5281/zenodo.6459795>.

413 The database of event-based effect sizes, surface properties and cyclone properties for each of the 1262 events (i.e.,
414 140 ± 41 unique tropical cyclones analysed for nine related definitions) can be accessed at:
415 <http://YYCdb.synology.me:5833/sharing/MqA4YFBHk>

416

417

418 **References**

419 Altman, J., Ukhvatkina, O. N., Omelko, A. M., Macek, M., Plener, T., Pejcha, V., Cerny, T., Petrik, P., Srutek, M.,
420 Song, J.-S., Zhmerenetsky, A. A., Vozmishcheva, A. S., Krestov, P.V., Petrenko, T. Y., Treydte, K., and Dolezal, J.:
421 Poleward migration of the destructive effects of tropical cyclones during the 20th century, Proc. Natl. Acad. Sci.,
422 115, 11543–11548, <https://doi.org/10.1073/pnas.1808979115>, 2018.

423 Barbier, E. B.: Economic aspects of tropical deforestation in Southeast Asia, *Glob. Ecol. Biogeogr. Lett.*, 3, 215,
424 <https://doi.org/10.2307/2997771>, 1993.

425 Beguería, S., Vicente-Serrano, S. M., Reig, F., and Latorre, B.: Standardized precipitation evapotranspiration index
426 (SPEI) revisited: Parameter fitting, evapotranspiration models, tools, datasets and drought monitoring, *Int. J.*
427 *Climatol.*, 34, 3001–3023, <https://doi.org/10.1002/joc.3887>, 2014.

428 Blanc, E. and Strobl, E.: Assessing the impact of typhoons on rice production in the Philippines, *J. Appl. Meteorol.*
429 *Climatol.*, 55, 993–1007, <https://doi.org/10.1175/jamc-d-15-0214.1>, 2016.

430 Bowen, T.: Social Protection in the Philippines “Emergency cash transfer” program in the Philippines, 1–16, 2016.

431 Bushnell, J. M., Cherrett, R. C., and Falvey, R. J.: Annual Tropical Cyclone Report 2018, 147pp., 2018.

432 Castañeda-Moya, E., Rivera-Monroy, V. H., Chambers, R. M., Zhao, X., Lamb-Wotton, L., Gorsky, A., Gaiser, E.
433 E., Troxler, T. G., Kominoski, J. S., and Hiatt, M.: Hurricanes fertilize mangrove forests in the Gulf of Mexico
434 (Florida Everglades, USA), *Proc. Natl. Acad. Sci. U. S. A.*, 117, 4831–4841,
435 <https://doi.org/10.1073/pnas.1908597117>, 2020.

436 Chambers, J. Q., Fisher, J. I., Zeng, H., Chapman, E. L., Baker, D. B., and Hurtt, G. C.: Hurricane Katrina’s carbon
437 footprint on U.S. Gulf coast forests, *Science*, 318, 1107–1107, <https://doi.org/10.1126/science.1148913>, 2007.

438 Chang, C.-T., Lee Shaner, P.-J., Wang, H.-H., and Lin, T.-C.: Resilience of a subtropical rainforest to annual
439 typhoon disturbance: Lessons from 25-year data of leaf area index, *For. Ecol. Manage.*, 470–471, 118210,
440 <https://doi.org/10.1016/j.foreco.2020.118210>, 2020.

441 Chen, Y.-Y., Gardiner, B., Pasztor, F., Blennow, K., Ryder, J., Valade, A., Naudts, K., Otto, J., McGrath, M. J.,
442 Planque, C., and Luyssaert, S.: Simulating damage for wind storms in the land surface model ORCHIDEE-CAN
443 (revision 4262), *Geosci. Model Dev.*, 11, 771–791, <https://doi.org/10.5194/gmd-11-771-2018>, 2018.

444 Chen, Y., Sharma, S., Zhou, X., Yang, K., Li, X., Niu, X., Hu, X., and Khadka, N.: Spatial performance of multiple
445 reanalysis precipitation datasets on the southern slope of central Himalaya, *Atmos. Res.*, 250, 105365,
446 <https://doi.org/10.1016/j.atmosres.2020.105365>, 2021.

447 Chiu, C.-M., Chien, C.-T., Nigh, G., and Chung, C.-H.: Influence of climate on tree mortality in Taiwan (Taiwania
448 *cryptomerioides*) stands in Taiwan, *New Zeal. J. For. Sci.*, 48, <https://doi.org/10.1186/s40490-018-0111-0>, 2018.

449 Choi, K.-S., Wu, C.-C., and Cha, E.-J.: Change of tropical cyclone activity by Pacific-Japan teleconnection pattern
450 in the western North Pacific, *J. Geophys. Res. Atmos.*, 115, 1–13, <https://doi.org/10.1029/2010JD013866>, 2010.

451 Choi, K.-S., Kim, D.-W., and Byun, H.-R.: Relationship between summer drought of mid-latitudes in East Asia and
452 tropical cyclone genesis frequency in the Western North Pacific, in: *Advances in Geosciences (A 6-Volume Set)*,
453 edited by: Satake, K. and Wu, C.-C., World Scientific Publishing Co. Pte. Ltd., 1–13,
454 https://doi.org/10.1142/9789814355315_0001, 2011.

455 Chou, C., Huang, L.-F., Tseng, L., Tu, J.-Y., and Tan, P.-H.: Annual cycle of rainfall in the Western North Pacific
456 and East Asian sector, *J. Clim.*, 22, 2073–2094, <https://doi.org/10.1175/2008JCLI2538.1>, 2009.

457 The Joint Typhoon Warning Center Tropical Cyclone Best-Tracks, 1945-2000:
458 <https://www.metoc.navy.mil/jtwc/products/best-tracks/tc-bt-report.html>, last access: 25June2019.

459 Curran, T. J., Brown, R. L., Edwards, E., Hopkins, K., Kelley, C., McCarthy, E., Pounds, E., Solan, R., and Wolf, J.:
460 Plant functional traits explain interspecific differences in immediate cyclone damage to trees of an endangered
461 rainforest community in north Queensland, *Austral Ecol.*, 33, 451–461, <https://doi.org/10.1111/j.1442->
462 9993.2008.01900.x, 2008.

463 Douglas, I.: Hydrological investigations of forest disturbance and land cover impacts in South–East Asia: a review,
464 *Philos. Trans. R. Soc. London. Ser. B Biol. Sci.*, 354, 1725–1738, <https://doi.org/10.1098/rstb.1999.0516>, 1999.

465 Dvorak, V. F.: Tropical cyclone intensity analysis using satellite data,
466 <https://repository.library.noaa.gov/view/noaa/19322>, 1984.

467 Dvorak, V. F., Smigielski, F. J., and States., U.: A workbook on tropical clouds and cloud systems observed in
468 satellite imagery, <file://catalog.hathitrust.org/Record/002715963>, 1990.

469 ECMWF: IFS Documentation CY45R1 - Part II : Data assimilation, in: IFS Documentation CY45R1, ECMWF,
470 <https://doi.org/10.21957/a3ri44ig4>, 2018.

471 ECMWF: ERA5-Land hourly data from 1981 to present, <https://doi.org/10.24381/cds.e2161bac>, 2019.

472 Eloy, C., Fournier, M., Lacoite, A., and Moulia, B.: Wind loads and competition for light sculpt trees into self-
473 similar structures, *Nat. Commun.*, 8, 1–11, <https://doi.org/10.1038/s41467-017-00995-6>, 2017.

474 ESA: Land Cover CCI Product User Guide Version 2, 105pp., 2017.

475 Forzieri, G., Pecchi, M., Girardello, M., Mauri, A., Klaus, M., Nikolov, C., Rüttschi, M., Gardiner, B., Tomaščík, J.,
476 Small, D., Nistor, C., Jonikavicius, D., Spinoni, J., Feyen, L., Giannetti, F., Comino, R., Wolynski, A., Pirotti, F.,
477 Maistrelli, F., Savulescu, I., Wurpillot-Lucas, S., Karlsson, S., Zieba-Kulawik, K., Strejcek-Jazwinska, P., Mokraš,
478 M., Franz, S., Krejci, L., Haidu, I., Nilsson, M., Wezyk, P., Catani, F., Chen, Y.-Y., Luysaert, S., Chirici, G.,
479 Cescatti, A., and Beck, P. S. A.: A spatially explicit database of wind disturbances in European forests over the
480 period 2000–2018, *Earth Syst. Sci. Data*, 12, 257–276, <https://doi.org/10.5194/essd-12-257-2020>, 2020.

481 Grice, J. W.: Computing and evaluating factor scores., *Psychol. Methods*, 6, 430–450, <https://doi.org/10.1037/1082->
482 989X.6.4.430, 2001.

483 Harris, I., Osborn, T. J., Jones, P., and Lister, D.: Version 4 of the CRU TS monthly high-resolution gridded
484 multivariate climate dataset, *Sci. Data*, 7, 1–18, <https://doi.org/10.1038/s41597-020-0453-3>, 2020.

485 Hersbach, H., Bell, B., Berrisford, P., Biavati, G., Horányi, A., Muñoz Sabater, J., Nicolas, J., Peubey, C., Radu, R.,
486 Rozum, I., Schepers, D., Simmons, A., Soci, C., Dee, D., Thépaut, J.-N. H. H., Bell, B., Berrisford, P., Biavati, G.,
487 and Horányi, A. J.-N.: ERA5 hourly data on single levels from 1959 to present. Copernicus Climate Change Service
488 (C3S) Climate Data Store (CDS), <https://doi.org/10.24381/cds.adbb2d47>, 2018.

489 Honkavaara, E., Litkey, P., and Nurminen, K.: Automatic storm damage detection in forests using high-altitude
490 photogrammetric imagery, *Remote Sens.*, 5, 1405–1424, <https://doi.org/10.3390/rs5031405>, 2013.

491 Jorge, S.-Z.: Copernicus Global Land Operations “Vegetation and Energy,”
492 https://land.copernicus.eu/global/sites/cgls.vito.be/files/products/CGLOPS1_SQE2019_LAI300m-V1_I1.00.pdf,
493 2020.

494 Kaplan, J. and Demaria, M.: On the decay of tropical cyclone winds after landfall in the New England Area, *J. Appl.*
495 *Meteorol.*, 40, 280–286, [https://doi.org/10.1175/1520-0450\(2001\)040<0280:OTDOTC>2.0.CO;2](https://doi.org/10.1175/1520-0450(2001)040<0280:OTDOTC>2.0.CO;2), 2001.

496 Kubota, H., Kosaka, Y., and Xie, S. P.: A 117-year long index of the Pacific-Japan pattern with application to
497 interdecadal variability, *Int. J. Climatol.*, 36, 1575–1589, <https://doi.org/10.1002/joc.4441>, 2016.

498 Landsea, C. W.: Climate variability of tropical cyclones: Past, Present and Future, in: *Storms*, edited by: Pielke, R.
499 A. S. and Pielke, R. A. J., Routledge, New York, 220–241, 2000.

500 Lin, T.-C., Hamburg, S., Lin, K.-C., Wang, L.-J., Chang, C.-T., Hsia, Y.-J., Vadeboncoeur, M. A., Mabry McMullen,
501 C. M., and Liu, C.-P.: Typhoon disturbance and forest dynamics: Lessons from a Northwest Pacific subtropical
502 forest, 14, 127–143, <https://doi.org/10.1007/s10021-010-9399-1>, 2011.

503 Lin, T. C., Hogan, J. A., and Chang, C. Te: Tropical Cyclone Ecology: A Scale-Link Perspective, *Trends Ecol. Evol.*,
504 35, 594–604, <https://doi.org/10.1016/j.tree.2020.02.012>, 2020.

505 Louf, J. F., Nelson, L., Kang, H., Song, P. N., Zehnbaauer, T., and Jung, S.: How wind drives the correlation between
506 leaf shape and mechanical properties, *Sci. Rep.*, 8, 1–7, <https://doi.org/10.1038/s41598-018-34588-0>, 2018.

507 Lu, Y., Yu, H., Yang, Q., Xu, M., Zheng, F., and Zhu, J.: Post-Disaster Survey of Typhoon Megi in Wenzhou City,
508 *Trop. Cyclone Res. Rev.*, 6, 34–39, <https://doi.org/10.6057/2017TCRRh1.04>, 2017.

509 ECMWF Confluence Wiki: Implementation of IFS cycle 45r1:
510 [https://confluence.ecmwf.int/display/FCST/Implementation+of+IFS+cycle+45r1#ImplementationofIFScycle45r1-](https://confluence.ecmwf.int/display/FCST/Implementation+of+IFS+cycle+45r1#ImplementationofIFScycle45r1-Tropicalcyclones)
511 *Tropicalcyclones*.

512 Mabry, C. M., Hamburg, S. P., Lin Teng-Chiu, Horng, F. W., King, H. B., and Hsia, Y. J.: Typhoon disturbance and
513 stand-level damage patterns at a subtropical forest in Taiwan, *Biotropica*, 30, 238–250,
514 <https://doi.org/10.1111/j.1744-7429.1998.tb00058.x>, 1998.

515 Martins, J. P., Trigo, I., and Freitas, S. C. de: Copernicus Global Land Operations "Vegetation and Energy"
516 "CGLOPS-1," *Copernicus Glob. L. Oper.*, 1–93, 2020.

517 McDowell, N. G., Allen, C. D., Anderson-Teixeira, K., Aukema, B. H., Bond-Lamberty, B., Chini, L., Clark, J. S.,
518 Dietze, M., Grossiord, C., Hanbury-Brown, A., Hurtt, G. C., Jackson, R. B., Johnson, D. J., Kueppers, L., Lichstein,
519 J. W., Ogle, K., Poulter, B., Pugh, T. A. M., Seidl, R., Turner, M. G., Uriarte, M., Walker, A. P., and Xu, C.:
520 Pervasive shifts in forest dynamics in a changing world, *Science*, 368, <https://doi.org/10.1126/science.aaz9463>, 2020.

521 Negrón-Juárez, R., Baker, D. B., Zeng, H., Henkel, T. K., and Chambers, J. Q.: Assessing hurricane-induced tree
522 mortality in U.S. Gulf Coast forest ecosystems, *J. Geophys. Res.*, 115, G04030,
523 <https://doi.org/10.1029/2009JG001221>, 2010.

524 Negrón-Juárez, R., Baker, D. B., Chambers, J. Q., Hurtt, G. C., and Goosem, S.: Multi-scale sensitivity of Landsat
525 and MODIS to forest disturbance associated with tropical cyclones, *Remote Sens. Environ.*, 140, 679–689,
526 <https://doi.org/10.1016/j.rse.2013.09.028>, 2014.

527 OCHA: Infrastructure Federation of Red Cross and Red Crescent Societies, Philippines : Typhoon Megi, 1–7pp.,
528 2010.

529 Ozdogan, M., Vladimirova, N., Radeloff, V. C., Krylov, A., Wolter, P. T., and Baumann, M.: Landsat remote
530 sensing of forest windfall disturbance, *Remote Sens. Environ.*, 143, 171–179,
531 <https://doi.org/10.1016/j.rse.2013.12.020>, 2014.

532 Rustad, L. E., Campbell, J. L., Marion, G. M., Norby, R. J., Mitchell, M. J., Hartley, A. E., Cornelissen, J. H. C.,
533 Gurevitch, J., Alward, R., Beier, C., Burke, I., Canadell, J., Callaghan, T., Christensen, T. R., Fahnestock, J.,
534 Fernandez, I., Harte, J., Hollister, R., John, H., Ineson, P., Johnson, M. G., Jonasson, S., John, L., Linder, S.,
535 Lukewille, A., Masters, G., Melillo, J., Mickelsen, A., Neill, C., Olszyk, D. M., Press, M., Pregitzer, K., Robinson,
536 C., Rygiewiez, P. T., Sala, O., Schmidt, I. K., Shaver, G., Thompson, K., Tingey, D. T., Verburg, P., Wall, D.,
537 Welker, J., and Wright, R.: A meta-analysis of the response of soil respiration, net nitrogen mineralization, and
538 aboveground plant growth to experimental ecosystem warming, *Oecologia*, 126, 543–562,
539 <https://doi.org/10.1007/s004420000544>, 2001.

540 Takao, G., Saigusa, N., Yamagata, Y., Hayashi, M., and Oguma, H.: Quantitative assessment of the impact of
541 typhoon disturbance on a Japanese forest using satellite laser altimetry, *Remote Sens. Environ.*, 156, 216–225,
542 <https://doi.org/10.1016/j.rse.2014.09.028>, 2014.

543 Tang, S., Lin, T.-C., Hsia, Y.-J., Hamburg, S. P., and Lin, K.-C.: Typhoon effects on litterfall in a subtropical forest,
544 *Can. J. For. Res.*, 33, 2184–2192, <https://doi.org/10.1139/x03-154>, 2003.

545 Therneau, T., Atkinson, B., and Ripley, B.: rpart: Recursive partitioning for classification, regression and survival
546 trees., CRAN R package version 4.1-15, 2019.

547 Uriarte, M., Thompson, J., and Zimmerman, J. K.: Hurricane María tripled stem breaks and doubled tree mortality
548 relative to other major storms, *Nat. Commun.*, 10, 1–7, <https://doi.org/10.1038/s41467-019-09319-2>, 2019.

549 Verger, A., Baret, F., and Weiss, M.: Near real-time vegetation monitoring at global scale, *IEEE J. Sel. Top. Appl.*
550 *Earth Obs. Remote Sens.*, 7, 3473–3481, <https://doi.org/10.1109/JSTARS.2014.2328632>, 2014.

551 Vickers, B., Kant, P., Bleaney, A., Milne, S., Suzuki, R., Ramos, L. T., Pohnan, E., and Lasco, R. D.: Forests and
552 Climate Change Working Paper 7: Forests and Climate Change in the Asia-Pacific Region, Food and Agriculture
553 Organization of the United Nations, Rome, 1–126pp., 2010.

554 Viro, E., Ponomarenko, A., Dehandschoewercker, Quéré, D., and Clanet, C.: Critical wind speed at which trees
555 break, *Phys. Rev. E*, 93, <https://doi.org/10.1103/PhysRevE.93.023001>, 2016.

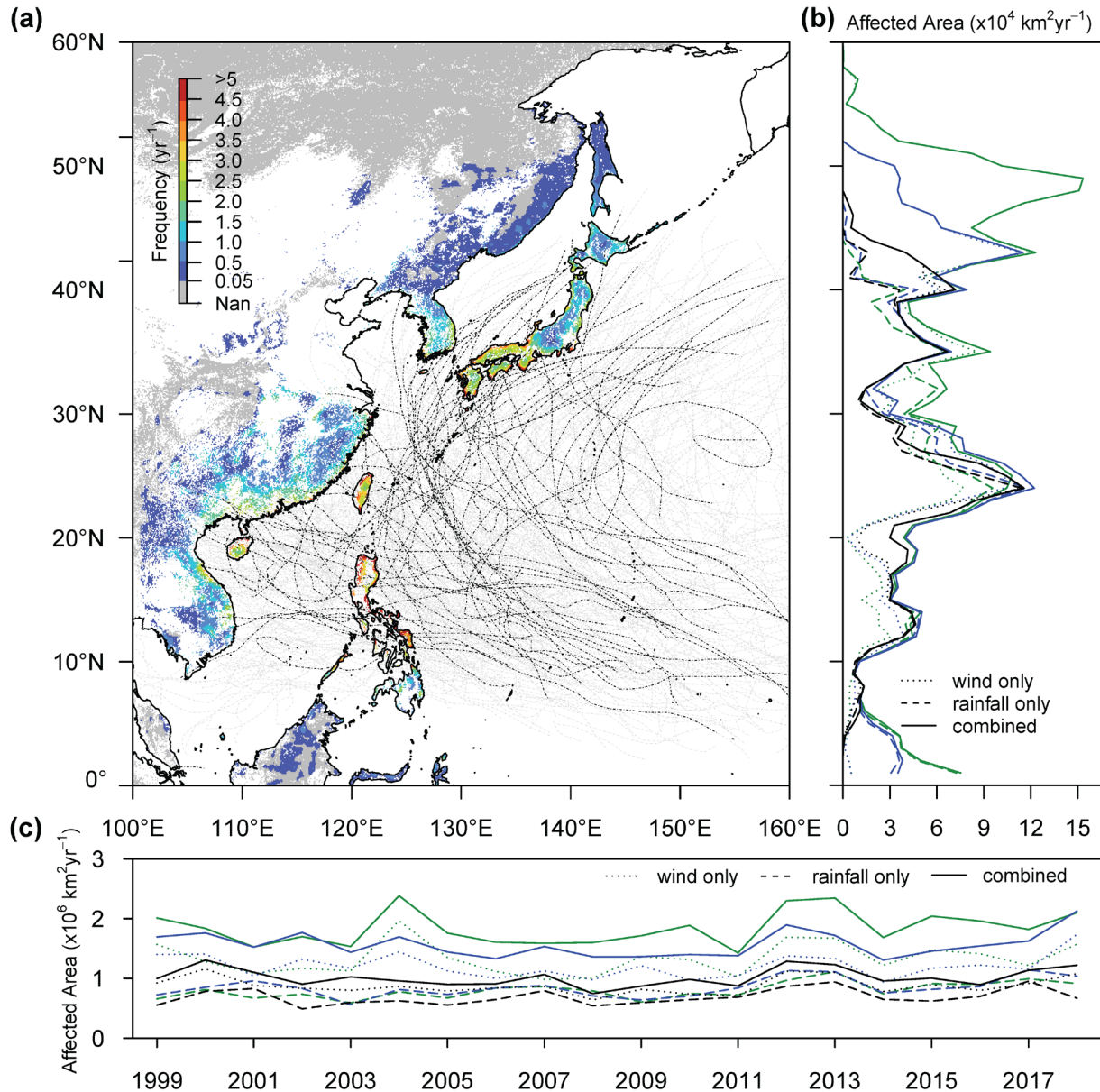
556 Wang, H.-C., Wang, S.-F., Lin, K.-C., Lee Shaner, P.-J., and Lin, T.-C.: Litterfall and Element Fluxes in a Natural
557 Hardwood Forest and a Chinese-fir Plantation Experiencing Frequent Typhoon Disturbance in Central Taiwan,
558 *Biotropica*, 45, 541–548, <https://doi.org/10.1111/btp.12048>, 2013.

559 Willoughby, H. E. and Rahn, M. E.: Parametric representation of the primary hurricane vortex. Part I: Observations
560 and evaluation of the Holland (1980) model, *Mon. Weather Rev.*, 132, 3033–3048,
561 <https://doi.org/10.1175/MWR2831.1>, 2004.

562 WMO: Global Guide to Tropical Cyclone Forecasting, 399pp., 2017.

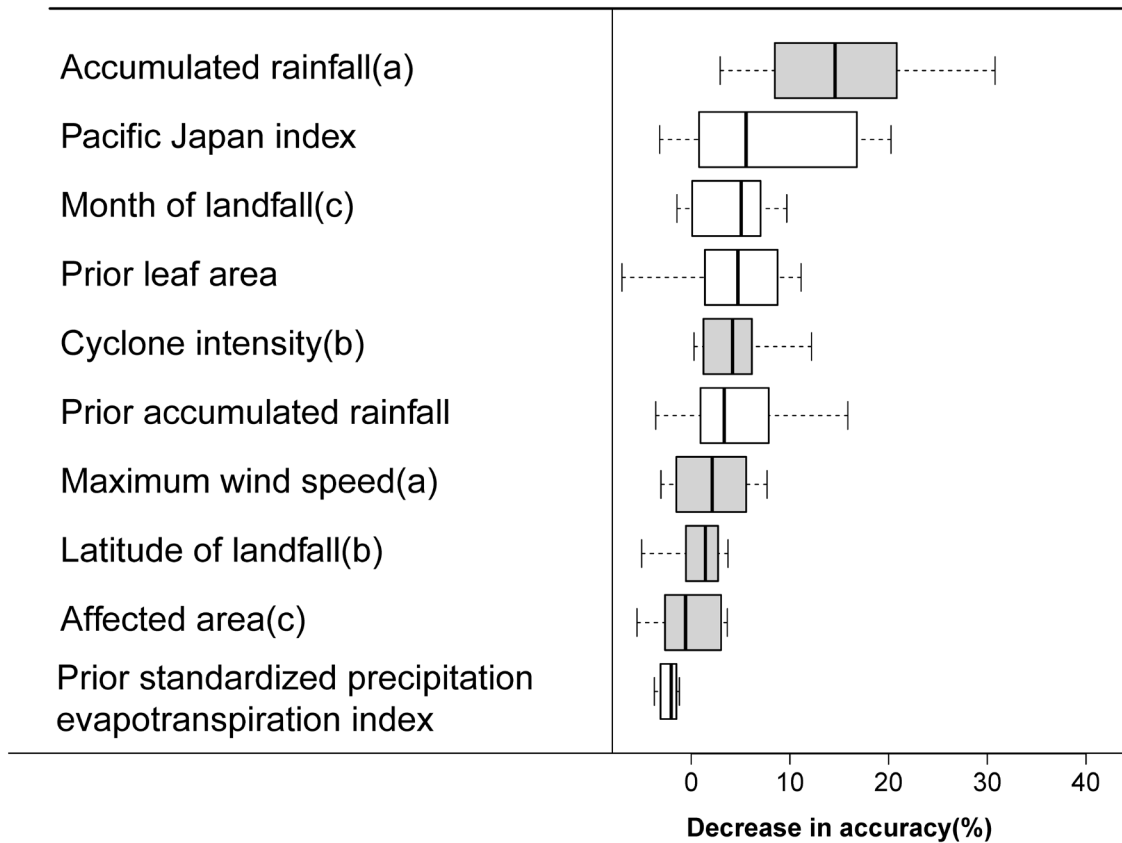
563 Xi, W.: Synergistic effects of tropical cyclones on forest ecosystems: a global synthesis, *J. For. Res.*, 26,
564 <https://doi.org/10.1007/s11676-015-0018-z>, 2015.

565 Yang, H.-H., Chen, S.-Y. C., Chien, S.-Y., and Li, W.-S.: Forensic Investigation of Typhoon Morakot Disaster:
566 Nansalu and Daniao Village Case Study (NCDR 102-T28), Taipei, 45pp., 2014.
567 Yoo, J., Kwon, H.-H. H., So, B.-J. J., Rajagopalan, B., and Kim, T.-W. W.: Identifying the role of typhoons as
568 drought busters in South Korea based on hidden Markov chain models, *Geophys. Res. Lett.*, 42, 2797–2804,
569 <https://doi.org/10.1002/2015GL063753>, 2015.
570



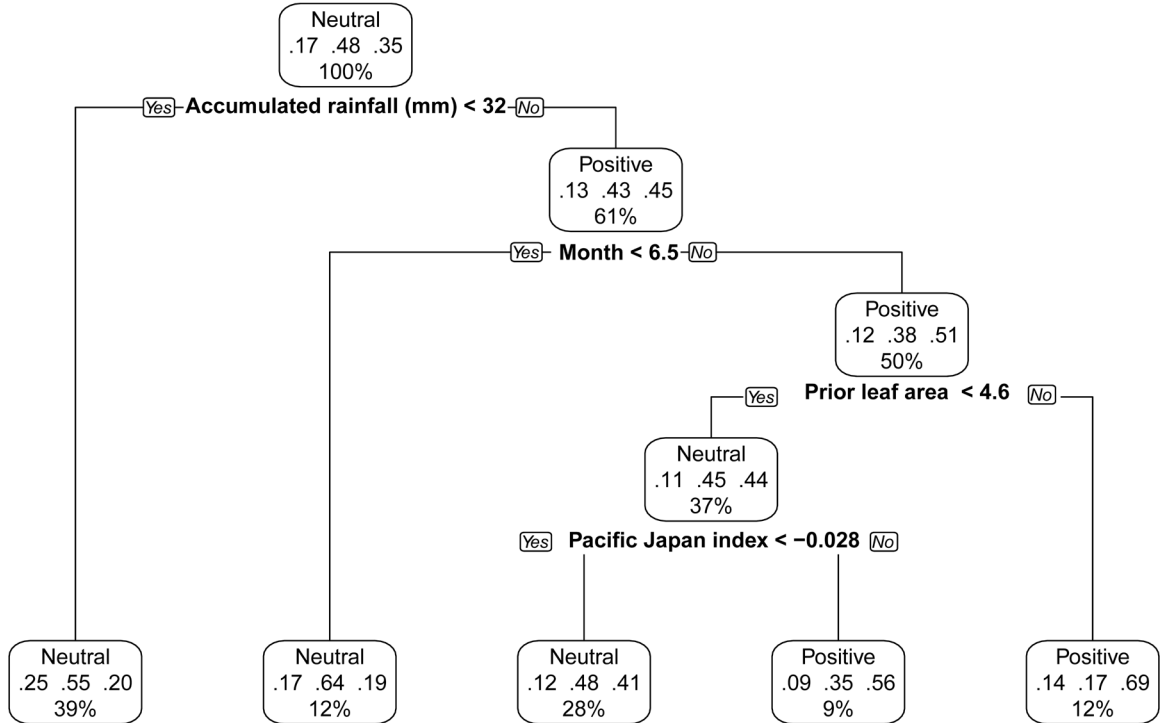
574 **Figure 1.** Spatial and temporal patterns of potential forest damage by tropical cyclones in East Asia. (a) Return
 575 frequency (yr^{-1}) of tropical cyclones between 1999 and 2018 following a combined wind-precipitation definition
 576 considering three diameters to define the width of the storm track (definition 3a in **Table A1**). Forests unlikely to
 577 have experienced a tropical cyclone between 1999 and 2018 are shaded in grey. For land locations shown in white,
 578 forest is not the dominant land cover. The dot-dashed lines show the cyclone tracks between 1999 and 2018. The
 579 black lines indicate the events that passed the quality control criteria used in this study. (b) Latitudinal gradients of
 580 potentially damaged forest area ($\text{km}^2 \text{yr}^{-1}$) between 1999 to 2018 for all nine definitions of affected area. Damage

581 potential is the outcome of an interplay between cyclone frequency, cyclone intensity, and the presence of forests.
582 The different definitions of affected area (**Table A1**) consistently show a high potential for forest damage over
583 island and coastal regions located between 10 and 35 degrees north. This high potential is largely driven by the
584 frequency of tropical cyclones (**Fig. A1**), i.e., two or more cyclones making landfall per year. Depending on how the
585 affected area is defined, there is a second region located between 40 and 50 degrees north with a high potential for
586 storm damage. In this region, the potential damage is the outcome of the high forest cover resulting in a strong
587 dependency on the assumed width of the storm track (**Fig. A1**). (c) Temporal dynamics of the total potentially
588 damaged forest area ($\text{km}^2 \text{yr}^{-1}$) for all nine definitions of affected area.
589



591
 592 **Figure 2.** Importance of five surface (white) and five cyclone (grey) characteristics in explaining the leaf area
 593 response to the passage of a tropical cyclone. The boxplots show the 95, 75, 50, 25 and 5 percentiles of the decrease
 594 in accuracy. The letters a, b and c following the label of a characteristic indicate collinearity between the variables
 595 (**Table A2**). Each boxplot contains the results of 12 random forest analyses fitted with different combinations of
 596 largely uncorrelated characteristics (**Table A3**). Each random forest analysis is based on 1262 cases coming from
 597 the 140 ± 41 individual tropical cyclones for which the impact was quantified according to nine related definitions
 598 (**Table A1**). The medians were used to sort the cyclone and surface characteristics according to decreasing
 599 importance.
 600

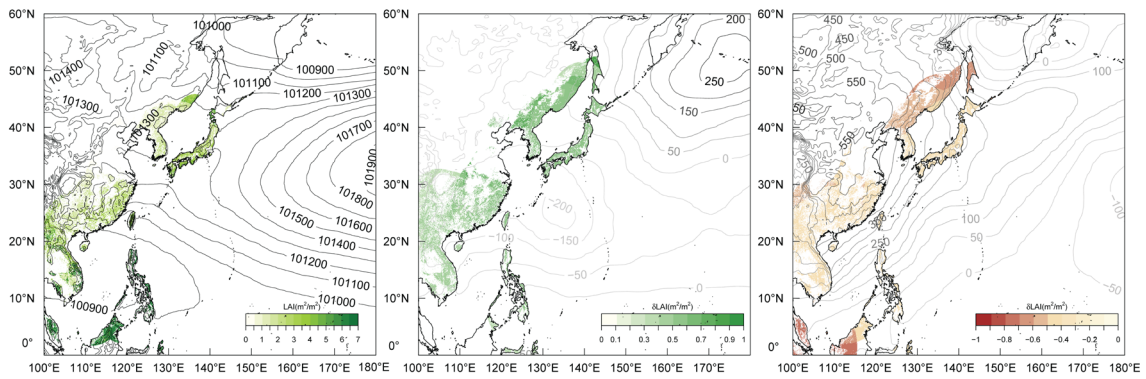
601



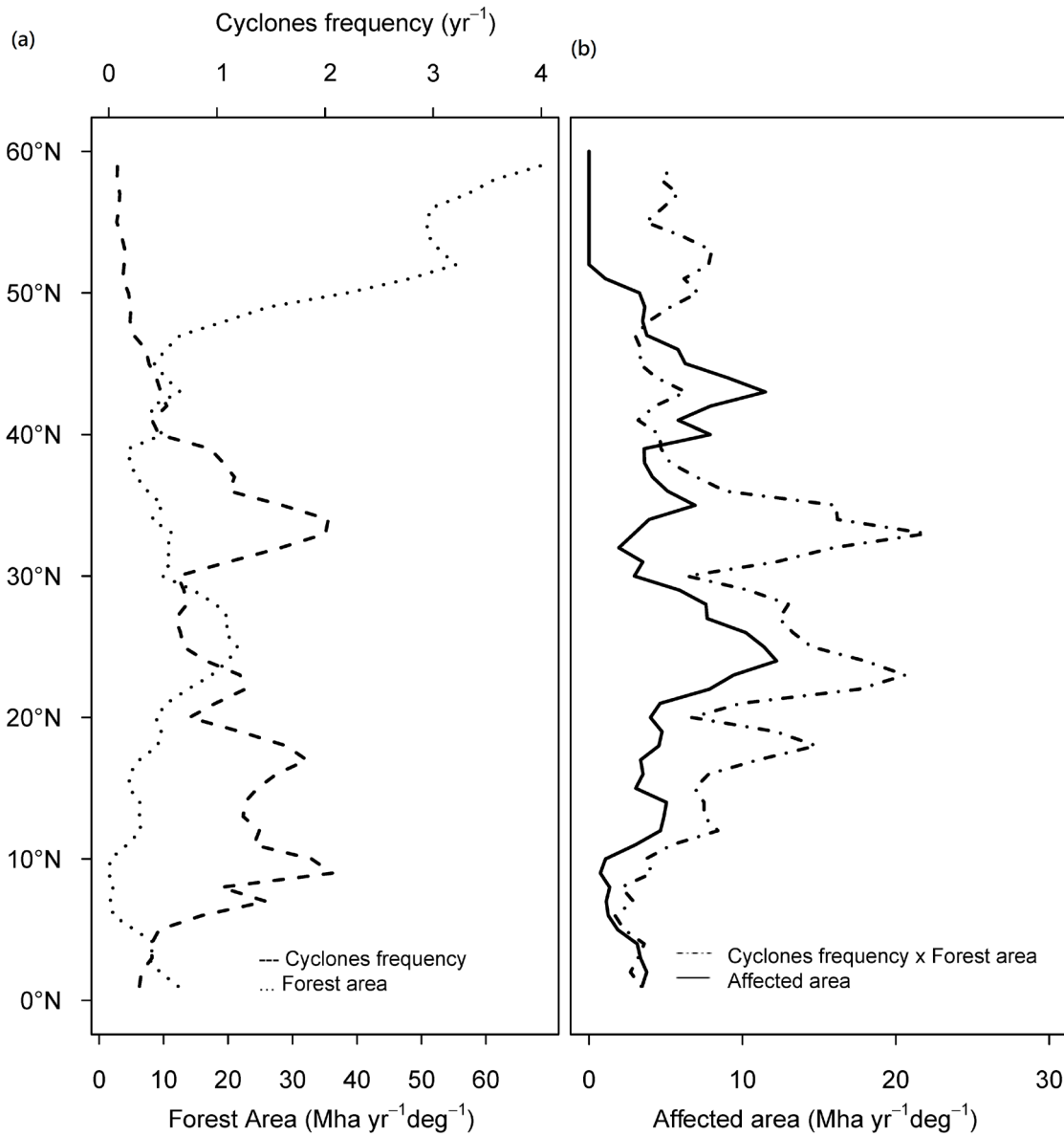
602

603 **Figure 3.** Environmental drivers contributing to an increase in leaf area in the affected compared to the reference
604 area, following the passage of a tropical cyclone. The fractions of a negative (left), neutral (middle) and positive
605 (right) effect size are shown in each box. The number of events is listed as the percentage of the total number of
606 events in the random tree (n=1262). To reduce the collinearity of the input variables, only the six variables with the
607 highest accuracy (**Fig. 2**) were used to create the four-layer decision tree.

608



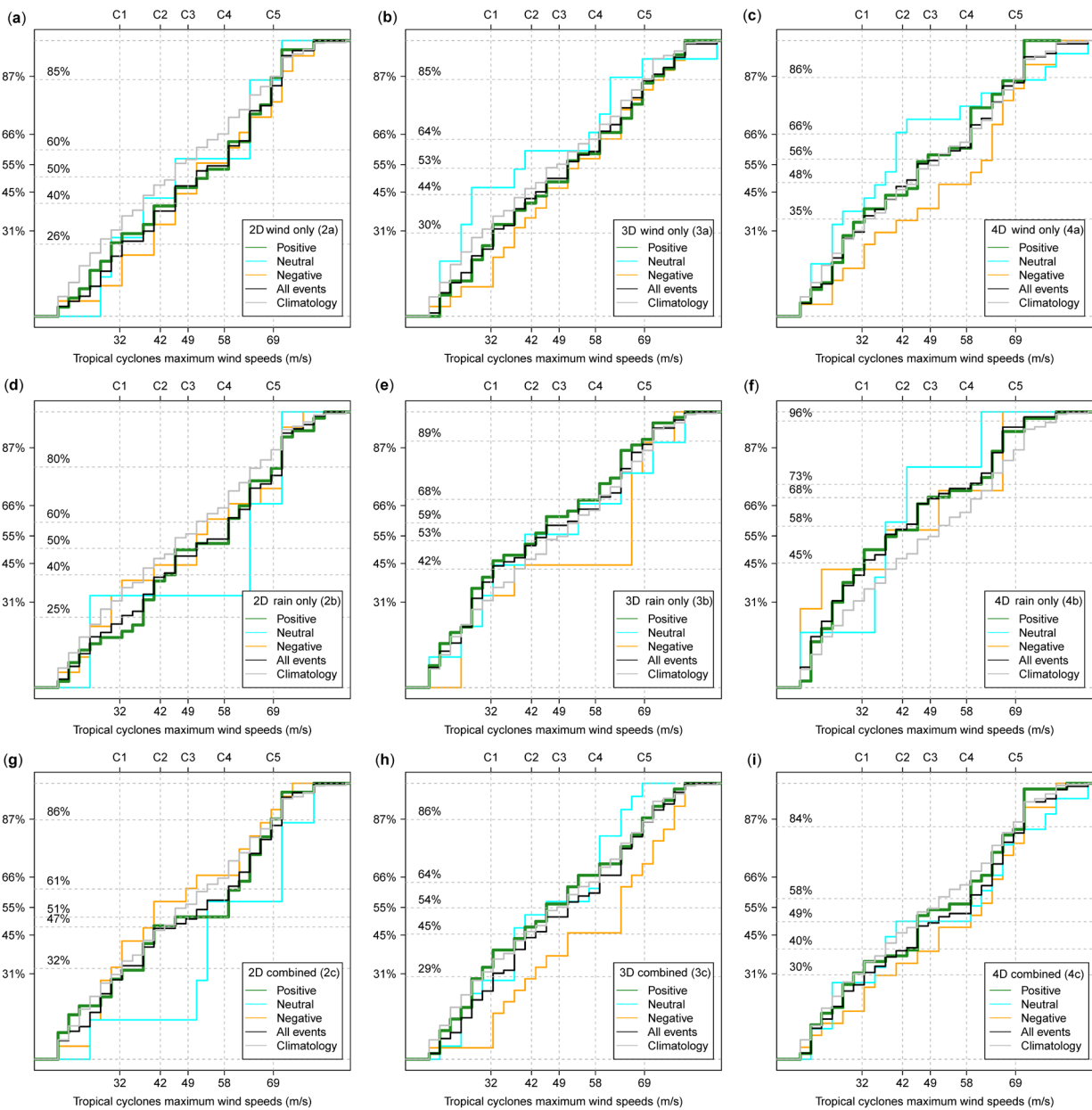
609
 610 **Figure 4.** Pressure fields (Pa) and changes therein in the month of the passage of a tropical cyclone for cyclones that
 611 had a neutral, positive, or negative impact on the leaf area ($\text{m}^2 \text{m}^{-2}$) of forests. Effect sizes are based on the definition
 612 that uses three times the cyclone diameter and wind speed to identify the affected and reference areas (definition 3a
 613 in **Table A1**) (a) Mean atmospheric pressure and leaf area prior to the passage of a tropical cyclone that had a
 614 neutral impact on forest leaf area. (b) Changes in mean atmospheric pressure and leaf area between cyclones with a
 615 neutral and positive effect on leaf area. (c) Changes in mean atmospheric pressure and leaf area between cyclones
 616 with a neutral and negative effect on leaf area.
 617



619

620 **Figure A1.** Contribution of return frequency and forest cover to the affected area: (a) zonal average of forest
 621 coverage (dotted line; km²) and the return frequency (dashed line; yr⁻¹) of tropical cyclones from 0 to 60 degrees N
 622 averaged over Eastern Asia, as defined in this study; (b) Zonal average of the interaction between return frequency
 623 and forest cover, calculated by multiplying the return frequency with the forest cover (dotdash line; km² yr⁻¹) and
 624 the estimated zonal average of the annual affected forest area (full line; km² yr⁻¹). Correlations between return
 625 frequency and affected area (Pearson correlation coefficient = -0.35, p-value < 0.01, n = 60), forest cover and
 626 affected area (Pearson correlation coefficient = 0.089, p-value = 0.5, n = 60) and frequency x cover and affected area

627 (Pearson correlation coefficient = 0.44, p-value < 0.01, n = 60). The latter thus correlates best with the zonal
628 variation in the affected area and was therefore shown in subplot b. Results are shown for affected areas defined as
629 locations within an area extending to three times the cyclone width for which the wind exceeded a threshold
630 (definition 3a in Table S1)
631



633

634

635

636

637

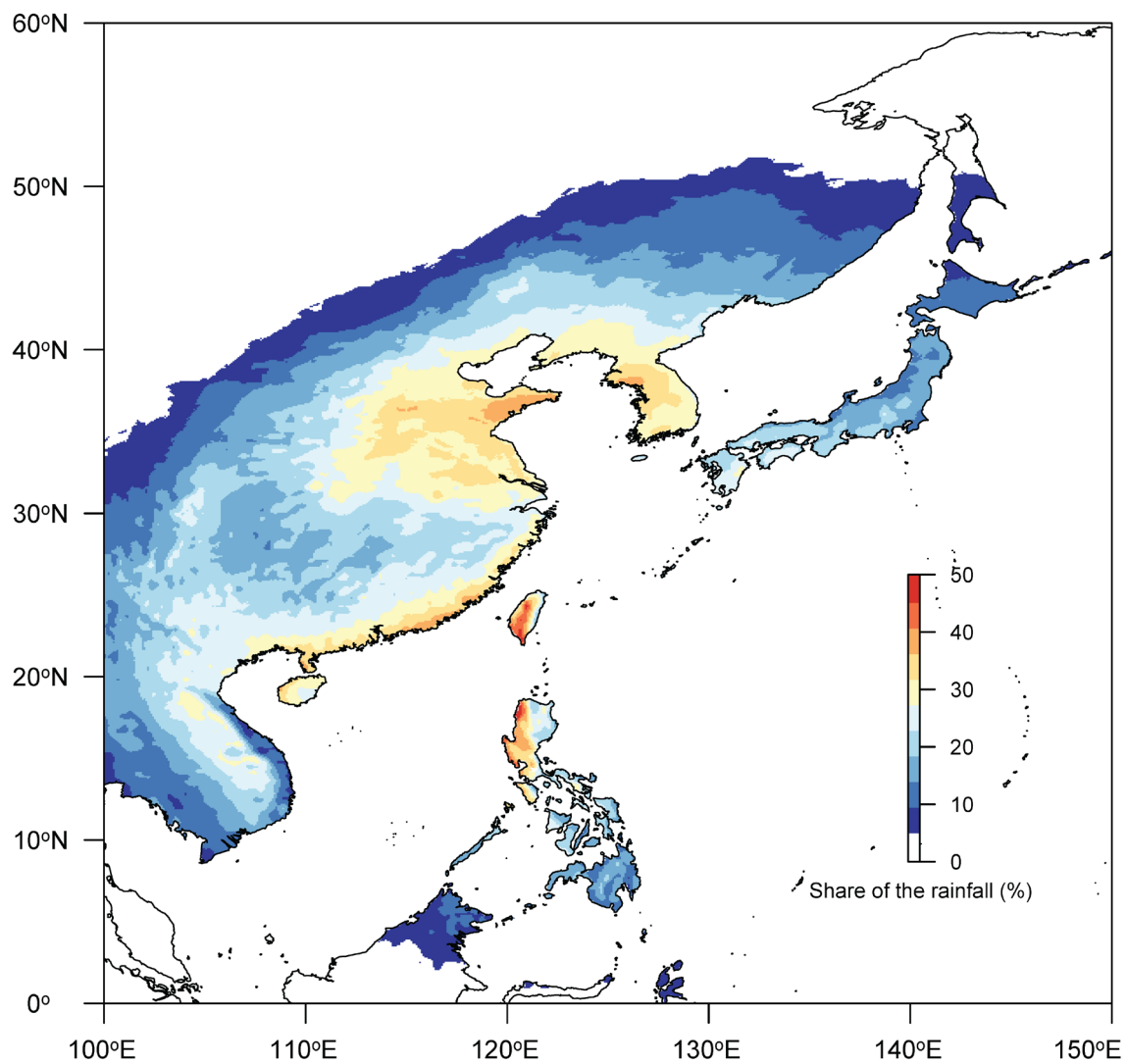
638

639

640

Figure A2. Cumulative distribution of tropical cyclones as a function of their maximum intensity for the nine definitions of affected area used in this study. The cumulative distribution for the census of 580 tropical cyclones recorded for the study period is shown left of the y-axis for class 1 (31%), class 2 (45%), class 3 (55%), class 4 (66%) and class 5 (87%) cyclones. The numbers shown of the right of the y-axis represent the cumulative distribution of the sample of the 580 events following a specific definition. Panel (a) shows wind only for 2 diameters, (b) wind only for 3 diameters, (c) wind only for 4 diameters, (d) rain only for 2 diameters, (e) rain only for 3 diameters, (f) rain only for 4 diameters, (g) wind or rain for 2 diameters, (h) wind or rain for 3 diameters, and (i) wind or rain for 4

641 diameters as detailed in Table S1. The intensity distribution for tropical cyclones with a negative effect size is shown
642 in orange, for tropical cyclones with a neutral effect size is shown in blue, and for tropical cyclones with a positive
643 effect size in green. The black solid line shows the distribution for the specific definition ($n = 140 \pm 41$ cyclones
644 depending on the definition). The grey solid line shows the distribution of the 580 events that occurred between
645 1999 to 2018. Small deviations between the grey and the black line suggest that the sample well represented the 580
646 cyclones in terms of their intensity class. The maximum wind speed of category 1 cyclones is between 32 m s^{-1} and
647 42 m s^{-1} , between 42 m s^{-1} and 49 m s^{-1} for category 2, between 49 m s^{-1} and 58 m s^{-1} for category 3, between 58 m s^{-1}
648 1 and 69 m s^{-1} for category 4, and exceeding 69 m s^{-1} for category 5. In East Asia, tropical cyclones of intensity class
649 3 or higher are called typhoons.
650



652

653 **Figure A3.** Share (%) of the rainfall contributed by tropical cyclones in June, July and August (JJA) to the total
654 annual rainfall over Eastern Asia between 1999 to 2018.

655 **Table A1.** Criteria for distinguishing between the affected and reference areas following the passage of an individual
656 cyclone and the number of events according to each specific definition. Group 1 groups definitions based on wind
657 speed, group 2 definitions are based on precipitation and group 3 definitions are based on both wind speed and
658 precipitation. All three definitions include an estimate of storm path based on a multiple of the reported storm
659 diameter. Column A denotes the number of events for which data were lacking so that the effect size could not be
660 calculated; column B denotes the number of events for which all required data were available; column C denotes the
661 subset of B for which the data passed the quality control; ES refers to effect size. A total of 580 unique tropical
662 cyclones were considered in this study.

Group	Affected area	Reference area	A	B	C	Negative effect size	Neutral effect size	Positive effect size
1.a	> 8 m s ⁻¹ and <2 diameters	< 8 m s ⁻¹ and <2 diameters	342	238	105	22	51	32
1.b	> 10 m s ⁻¹ and <3 diameters	< 10 m s ⁻¹ and <3 diameters	305	275	182	38	97	47
1.c	> 12 m s ⁻¹ and <4 diameters	< 12 m s ⁻¹ and <4 diameters	291	289	183	31	92	60
2.a	> 60 mm and <2 diameters	< 60 mm and <2 diameters	338	242	115	19	51	45
2.b	> 80 mm and <3 diameters	< 80 mm and <3 diameters	315	265	129	11	59	59
2.c	> 100 mm and <4 diameters	< 100 mm and <4 diameters	311	269	86	9	32	45
3.a	(> 8 m s ⁻¹ or > 60 mm) and <2 diameters	(< 8 m s ⁻¹ or < 60 mm) and < 2 diameters	352	228	103	25	45	33
3.b	(> 10 m s ⁻¹ or > 80 mm) and <3 diameters	(< 10 m s ⁻¹ or < 80 mm) and < 3 diameters	304	276	188	38	95	55
3.c	(> 12 m s ⁻¹ or > 100 mm) and <4 diameters	(< 12 m s ⁻¹ or < 100 mm) and < 4 diameters	288	292	171	35	83	53
Mean			316	264	140	25	67	48
Std			22	22	41	11	25	10
Mean (%)			54	46	24	18	48	34
Std (%)			4	4	7	8	18	7

663

664

665 **Table A2.** Loadings of each characteristic on three axes and collinearity between variables within the same group.
 666 Collinearity was used to build random forests with largely uncorrelated explanatory variables (**Fig. 2 & 3**). Factor
 667 analysis was performed separately for each group. Given the exploratory nature of this analysis, a factor loading of
 668 0.6 was used as a cut-off and those exceeding that level are highlighted in bold face.
 669

Group	Characteristics	FC1	FC2	FC3	Collinearity
Cyclone characteristics	Maximum wind speed during passage over land (m s ⁻¹)	0.01	-0.79	0.21	a
	Accumulated rainfall during passage over land (mm)	-0.18	-0.83	-0.03	a
	Latitude of landfall (degrees)	0.83	0.04	0.08	b
	Intensity of the tropical cyclone, gusts (m s ⁻¹)	0.87	0.14	0.06	b
	Affected area during passage over land (ha)	0.15	0.09	0.97	c
Surface conditions prior to the cyclone	Month of landfall	-0.35	-0.06	0.72	c
	Prior accumulated rainfall (30 days prior to landfall (mm))	0.62	0.60	0.17	d
	Prior leaf area index (30 days prior to landfall (m ² m ⁻²))	0.87	-0.06	-0.07	e
	Prior Pacific Japan index (Pa Pa ⁻¹)	-0.69	-0.07	0.74	f
	Prior drought state (standardized precipitation and evapotranspiration index, 30 days prior to landfall (mm mm ⁻¹))	0.01	0.95	0.03	g

670

671 **Table A3.** Sets of largely independent variables that were used as input in the random forest analysis. Details of the
672 variables are given in the section “multivariate analysis”. The justification for the groups is given by the collinearity
673 as reported in Table S2.
674

Set	Group with tropical cyclone characteristics	Group with land characteristics prior to the cyclone
1	Maximum wind speed, latitude & affected area	Month & prior accumulated rainfall
2	Maximum wind speed, cyclone intensity & affected area	Prior accumulated rainfall, prior leaf area, & prior standardized precipitation and evapotranspiration index
3	Accumulated rainfall, latitude & affected area	Prior Pacific Japan index & prior standardized precipitation and evapotranspiration index
4	Accumulated rainfall, cyclone intensity & affected area	